SUSAN 3D CHARACTERIZATION FOR MANUFACTURED CYLINDER EDGE DETECTION

Nicolas Walter, Olivier Aubreton, Olivier Laligant

Laboratoire Le2i, 12, rue de la fonderie, Le Creusot, France.

ABSTRACT

This paper deals with edge detection and vertex characterization of 3D meshes. First, the 2D SUSAN principle is reminded. The relationship between the saliency degree and the curvature is recalled for continuous and discontinuous 2D curves. A description of the operator for 3D meshes is given, which directly provides the shape information for a vertex of a mesh without any curvature computation. To assess the technique, a strategy of comparison between the SUSAN 3D operator and a curvature operator (Meyer [1,2]) is detailed. Results are shown for a real manufactured object. To conclude, we present advantages and drawbacks of the SUSAN 3D operator and give perspectives for future works. The contributions of this work are the definition of a comparison method between the SUSAN 3D operator and curvature operators, and an application for edge detection on a real cylinder.

Keyword list: 3D Salient point detection, saliency degree measurement, point/vertex characterization, SUSAN 3D

1. Introduction

Nowadays, one of the most important research topics, in the broad domain of 3D data analysis, is the characterization of 3D points. Indeed, as expressed Y.K. Lai et al. [5]: "Sharp edges, ridges, valleys, and prongs are critical for the appearance and accurate representation of a 3D model." Most recent techniques are based on curvature analysis, and have been applied to different types of meshes. Based on the work and state of the art established by D.L. Page et al. [8], two operator classes can be summarized:

- Operators based on curvature analysis, classified into three types: SFM [11], TCM [2], and CFM [15].
- 2D operators extended to 3D data or operators that adapt the 3D data for 2D operators.

For not sufficiently smooth meshes, or in the presence of a discontinuity, operators based on curvature analysis can not compute the curvature, because of its definition. Y.K. Lai et al. [5], D.L. Page et al. [8], M. Meyer et al. [2] and others assume that the surface is sufficiently smoothed to apply theirs operators. Moreover, the presence of a sharp edge often infers additional computations. The method presented in this article belongs to the second class of operators, and propose a direct extension of the 2D SUSAN operator for regular or irregular triangle meshes.

2. Recall on the SUSAN 2D principle

SUSAN method [13] is based on a circular window in which the center pixel, named nucleus, is the analyzed pixel. A pixel attribute is then chosen, for example the grey level in 2D images. In the circular window, the USAN area is defined as the set of pixels presenting a close value (bounded by a threshold) to the nucleus attribute. The operator response is the ratio of the USAN area over the total area of the circular window. In this way, a salient point corresponds to a minimum response of the SUSAN operator. We named the response of the SUSAN operator the saliency degree.

3. Relation between the saliency degree and the curvature

It can be demonstrated [17] for a 2D continuous form (the edge curve of an object), and represented as a parabolic form by $f(x) = ax^2$, that the relation between the 2D saliency degree and the curvature is ruled by the expression:

$$S_d = \frac{A_{USAN}}{\pi R^2} = \frac{1}{2} + \frac{\kappa(d_2^{\,3} - d_1^{\,3})}{6\pi R^2} + \frac{\alpha}{\pi} - \frac{\sin(2\alpha)}{2\pi} \qquad (1)$$

With $d_1 = -\sqrt{\frac{2\sqrt{1+\kappa^2 R^2}-2}{\kappa^2}} = -d_2$, $\alpha = \arctan\left(\frac{\kappa d_2}{2}\right)$, κ = κ(0) =2a at the vertex C_0 and S_d ϵ]0, 1[.

For a fixed observation radius R, the saliency degree only depends on the parameter a and thus on the curvature. We can observe the evolution of the saliency degree in function of the curvature evolution on Figure 2.:

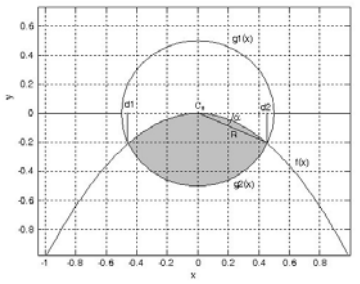

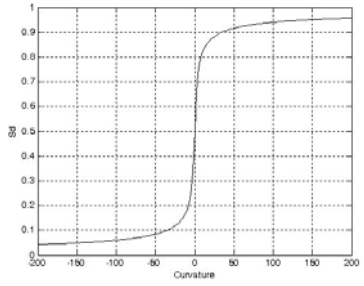

Fig.1. Intersection of a circular window and a sufficiently smooth surface with $f(x)=-x^2$ and R=0,5 at C_0.
Fig.2. Evolution of the saliency degree in function of the curvature.

Similarly, for a 2D discontinuous form represented by $f(x) = b|x|$, the relation between the 2D saliency degree and the parameter *b* is ruled by the equation:

$$S_d = \frac{A_{USAN}}{\pi R^2} = \frac{1}{2} + \frac{\alpha}{\pi} \qquad (2)$$

with $\alpha = \arctan(b)$ and S_d ϵ]0, 1[.

For a fixed observation radius R, the saliency degree depends only on the parameter *b*. We can observe the evolution of the saliency degree in function of the curvature evolution on Figure 4.:

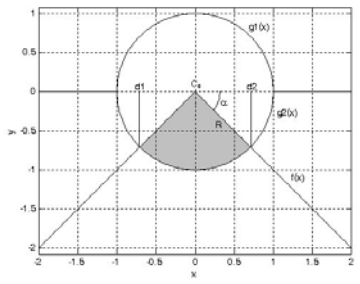

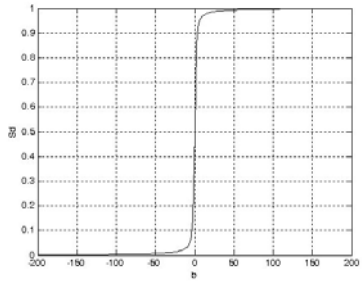

Fig.3. Intersection of a circular window and a non sufficiently smooth surface with $f(x)=-|x|$ and R=1 at C_0.
Fig.4. Evolution of the saliency degree in function of the parameter *b*.

The saliency degree is defined for the continuous and discontinuous domain. Three types of edges can be extracted by the response of this operator. The S_d value can be used directly to classify a vertex as a salient, flat or cavity point.

4. SUSAN operator extension for meshes

The evolution of the saliency degree can be observed for a circular window centered at C_0. Indeed, we are interested to apply this principle to detect salient points on a 3D mesh. A mesh always describes the edge of an object or a part of an object. At a point of the mesh on a sufficiently smooth surface, the SFM techniques extract the curvature by integration, as described by D.L. Page [8]. It is also expressed by M. Meyer et al. [2] as "for every unit direction e_θ in the tangent plane, the normal curvature $\kappa^N(\theta)=\kappa_1\cos^2(\theta)+\kappa_2\sin^2(\theta)$, defined as the curvature of the curve that belongs to both the surface itself and a perpendicular plane containing both the normal vector and e_θ." The mean curvature $\overline{\kappa}$ is then defined as the average of the normal curvatures in every e_θ directions:

$$\overline{\kappa} = \int_0^{2\pi} \kappa^N(\theta)\, d\theta \qquad (3)$$

As proven above, the saliency degree is related to the curvature for sufficiently smoothed surfaces. By analogy, Figures 1 and 3 can be viewed as a visualization of a tangent plane at the point C_0. The saliency degree can be

computed in every direction e_θ. Then, we define for a 3D model a mean saliency degree. At a point of a mesh $\overline{S_d}$ can be expressed by:

$$\overline{S_d} = \int_0^{2\pi} S_d{}^N(\theta) d\theta \tag{4}$$

Where the normal saliency degree could be defined as $S_d^N(\theta)=S_d^1\cos^2(\theta)+ S_d^2\sin^2(\theta)$, with S_d^1 and S_d^2 the principal saliency degrees of the surface at C_0, and e_1 and e_2 the orthogonal principal directions of saliency. The computation of the mean curvature is not possible in the presence of a discontinuity, but the mean saliency degree will always give a coherent result. The mean saliency degree computation, due to the isotropy of the circular analysis window in the e_θ directions, depends on the volume intersection of a sphere and the surface around the inspected point. The homologous 3D operator to a circular pixellized window is a voxellized sphere. At a point of a mesh, the mean saliency degree is computed by determining the USAN volume. The nucleus of the voxellized sphere is defined as the center of gravity of the central voxel weighted by its volume. All voxels are defined as a point and a weight. By centering the nucleus at a point of the mesh, and defining the attribute of voxels under or on the surface as 1, the USAN volume can be determined by summing the weight of the voxels of the sphere that are under the surface (see Figure 5). The saliency degree is finally defined by:

$$\overline{S_d} = \frac{V_{USAN}}{V_{Sph.Vox}} \tag{5}$$

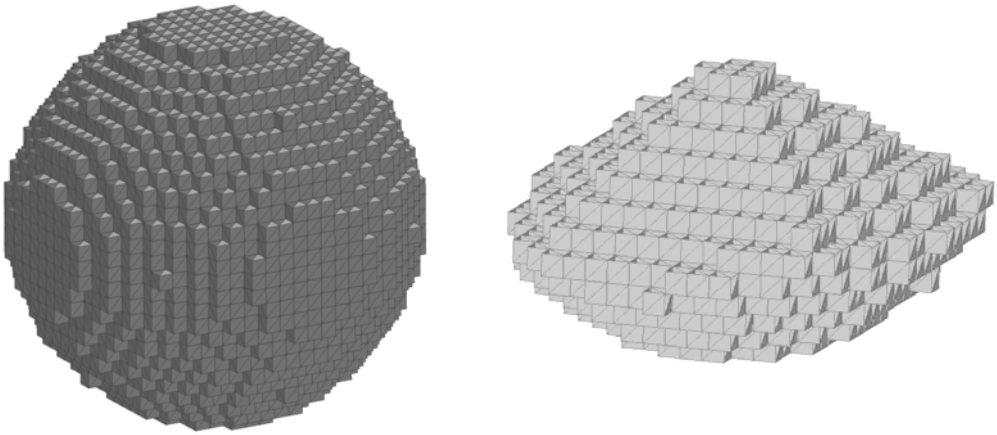

Fig. 5. On the left, a voxellization example of a sphere. On the right, example of an extracted USAN volume

5. Method to compare results

To assess the technique, the first idea is to compare directly the results of the SUSAN 3D, the saliency degree $\overline{S_d}$, with the results of the Meyer [1,2] operator, the mean curvature $\overline{\kappa}$, but the comparison is not consistent. A simple strategy to compare the results of the operators consist in the use of principal curvatures extracted by the Meyer operator [1,2]. Indeed, the mean curvature can be deduced from the principal curvatures by the formula:

$$\overline{\kappa} = \frac{\kappa_1 + \kappa_2}{2} \tag{6}$$

The advantage of using this formula is that the formula (1) can be applied on each principal curvatures, and the $\overline{S_d}$ can be deduced. Once the two responses of the operators are in the same comparison space, the saliency degree space, they can be compared.

6. Evaluation of the method on a simple example

To quantify the efficiency of our technique, we present a table of standard deviations, in the Figure 6, computed on three spheres of the same radius (R_{Sph} = 3), with pseudo-regular and irregular meshes and different resolutions: 1280, 5120 and 20480 faces. For each sphere, the radius (R_{SUSAN}) of the SUSAN 3D operator is unique. In order to respect the width of the Meyer operator [1,2] that is restricted to the 1Ring, the radius of the SUSAN 3D operator is chosen in function of the distances of the firsts vertices of the 1Ring. The curvature at each vertex in each principal direction on a sphere is the same depending only on the radius of the sphere studied. At each vertex, the mean curvature is equivalent to:

$$\overline{\kappa} = \frac{\kappa + \kappa}{2} = \kappa = \frac{1}{R_{Sph}} \tag{7}$$

Finding the mean curvature at a vertex of a sphere is equivalent to find the mean curvature of a 2D parabolic form at C_0. The equivalent mean curvature of the two forms is: $\bar{\kappa} = 2a = \frac{1}{R_{Sph}}$.

	Saliency degree errors	Saliency degree errors obtained from the Meyer operator
Sphere 1280 regular faces with R_{SUSAN} = 0.5	2.6156e-002	1.67309e-006
Sphere 5120 regular faces with R_{SUSAN} = 0.25	1.3036 e-002	3.17554e-006
Sphere 20480 regular faces with R_{SUSAN} = 0.125	6.563 e-003	6.44562e-006
Sphere 1280 irregular faces with R_{SUSAN} = 0.46	2.8418 e-002	2.33877 e-003
Sphere 5120 irregular faces with R_{SUSAN} = 0.24	1.7018 e-002	2.73231 e-003
Sphere 20480 irregular faces with R_{SUSAN} = 0.119	1.0228 e-002	2.80958 e-003

Fig.6. Comparison of standard deviation errors of saliency degrees obtained on three synthetics spheres with regular and irregular meshes.

We must underline that surfaces of the created spheres are well smoothed and our operator is dedicated to non smoothed surfaces, that's why results above are better with the Meyer [1,2] operator. Moreover, standard deviations, with our operator, are more stable and less dependant on the mesh quality or regularity. We must underline that the precision of our operator depend on the decomposition level of the voxellized sphere. The results are obtained with a third decomposition level of a 27tree algorithm [18].

7. Application on a manufactured cylinder

The dimensional measure of manufactured objects is one of the problematic at our laboratory and specifically the measure of the radii of cylinders for quality control. The manufactured cylinder studied is an object of great size and has been scanned on the production line. The operator described in this paper is well suited to detect edges of this type of objects. Indeed, the noise generated by the scanner during the acquisition step has a great influence on results obtained with the Meyer [1,2] operator that is limited in width to the 1Ring. On the contrary, the width of our operator is not limited to the 1Ring and the responses on discontinuities due to the noise are always reliable. The results shown below is a comparison in the saliency space, between results of our operator and the Meyer operator:

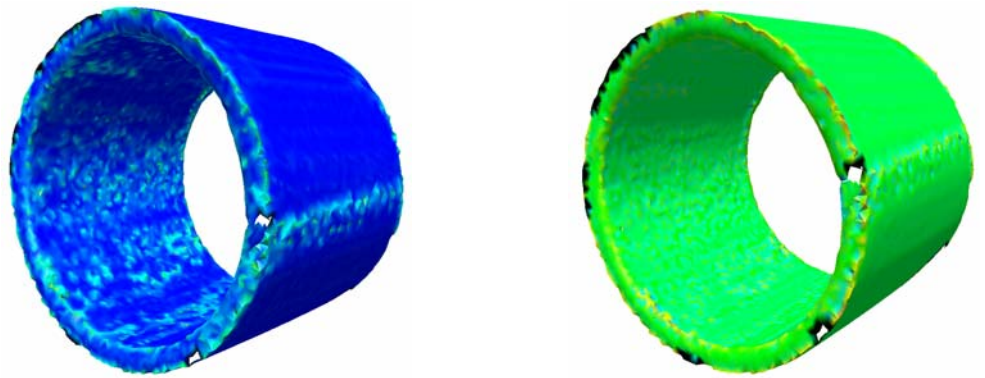

Fig.7. Left, Saliency degree results on a manufactured cylinder, obtained form the Meyer operator. Right, Results of saliency degrees obtained on the same cylinder with our SUSAN 3D operator with radius corresponding to the mean distance of first vertices of the1Ring in the whole mesh.

As benefits and drawbacks, with help of figure 7 and 8, we can infer that our operator differentiate discontinuous edges more than the Meyer operator. We must underline that Meyer operator is well suited for regular and well smoothed meshes, that is not the case here. An other advantage of our operator is that the width of our operator can be extended to more than a 1Ring (see Figure 8). As shown by Figure 6, our operator is less precise than the Meyer operator, but the results are less sensible to the regularity of the mesh. Moreover, the precision of our operator depends only on the decomposition level of the voxellized sphere. We can refine the precision by

decomposing the sphere on the superior level. Analysing the mesh with a greater radius will also enhance the detected edges.

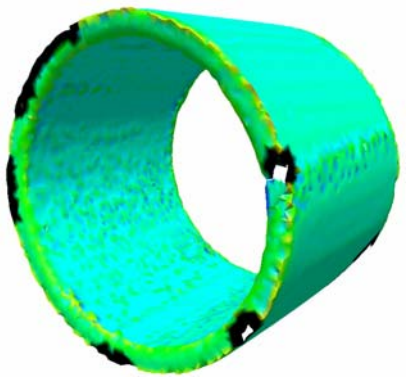

Fig.8. Saliency degree results on the same cylinder with our SUSAN 3D operator with a radius two times larger than the radius of the Figure 7.

8. Conclusion

In this article, we have shown that our operator is reliable on discontinuous and continuous form and is slight sensible to the regularity of the mesh. Drawback is the lack of precision on smoothed surfaces due to the weak sampling of the volume in 3D. Future works are naturally focused on the comparison of our operator with operators that are not limited to the 1Ring, like feature sensitive operators [5 or 16]. The extraction of principal saliency degrees and directions will be also studied as well as the influence of the noise on the characterization.

9. References

[1] Meyer, M., Desbrun, M., Schröder, P., Barr, A.H., “Implicit fairing of irregular meshes using diffusion and curvature flow,” Computer Graphics Proceedings (SIGGRAPH'99), 317-324 (1999).

[2] Meyer, M., Desbrun, M., Schröder, P., Barr, A.H., “Discrete differencial-geometry operators for triangulated 2-manifolds,” VisMath (2002).

[3] Fournier, M., Dischler, J.M., Bechmann, D., “Filtrage adaptatif des données acquises par un scanner 3D et représentées par une transformée en distance volumétrique,” AFIG days, J.C. Gonzato, J.P. Jessel (Editors). Bordeaux, (2006).

[4] Loriot, B., Fougerolle, Y., Sestier, C., Seulin, R., “3D acquisition and modeling for flint artefacts analysis,” SPIE Optical Metrology – Optics for AAA, Germany (2007).

[5] Lai, Y.K., Zhou, Q.Y., Hu, S.M., Wallner, J., Pottmann, H., “Robust Feature Classification and Editing,” IEEE Transaction on visualisation and computer graphics, 13 (1), 34-45, (2007).

[6] Mao, Z., Ma, L., Zhao, M., Xiao, X., “SUSAN structure preserving filtering for mesh denoising,” The Visual Computer vol. 22, pp. 276-284, © Springer–Verlag (2006).

[7] Monga, O., Deriche, R., “3D edge detection using recursive filtering: Application to scanner images,” INRIA Research report number 930, Program 6, (1988).

[8] Page, D.L., Sun, Y., Koschan, A.F., Paik, J., Abidi, M.A., “Normal vector voting: Crease detection and curvature estimation on large noisy meshes,” Graphical Models, 64 (3-4), 199-229, © Elsevier Science (2002).

[9] Pinkall, U., Polthier, K., “Computing discrete minimal surfaces and their conjugates,” Experimental Mathematics, 2 (1), 15-36, © A K Peters, Ltd (1993).

[10] Polthier, K., Schmies, M., “Straightest geodesics on polyhedral surfaces,” Mathematical Visualization , 391-409, © Springer-Verlag (1998).

[11] Pulla, S., Razdan, A., Farin, G., “Improved curvature estimation for watershed segmentation of 3D meshes,” Manuscript (2001).

[12] Rössl, C., Kobbelt, L., Seidel, H.P., “Extraction of feature lines on triangulated surfaces using morphological operators,” Smart Graphics (AAAI Symposium), 71-75, AAAI Press (2000).

[13] Smith, S.M., Brady, J.M., “Susan – A new approach to low level image processing,” International Journal of Computer Vision, 23 (1), 45-78, © Kluwer Academic Publishers (1997).

[14] Tang, C.K., Medioni, G., “Robust estimation of curvature information from noisy 3D data for shape description,” Proceedings of the Seventh International Conference on Computer Vision, 426-433, Kerkyra, Greece (1999).

[15] Taubin, G., “Estimating the tensor of curvature of a surface from a polyhedral approximation,” Proceedings of the Fifth International Conference on Computer Vision, pp. 902-907, © IEEE computer society (1995).
[16] Clarentz, U., Griebel, M., Rumpf, M., Schweitzer, M.A., Telea, A., “Feature sensitive editing on surfaces,” The Visual Computer (2004).
[17] Walter, N., Aubreton, O., Laligant, O., “Salient point characterization for low resolution meshes,” IEEE International Conference on Image Processing (2008).
[18] Walter, N., Aubreton, O., Laligant, O., “Salient Point SUSAN 3D operator for triangles meshes,” The 2nd International Topical Meeting on Optical Sensing and Artificial Vision, Saint-Petersburg, Russia (2008).